

Supplement of Atmos. Chem. Phys., 15, 973–990, 2015
<http://www.atmos-chem-phys.net/15/973/2015/>
doi:10.5194/acp-15-973-2015-supplement
© Author(s) 2015. CC Attribution 3.0 License.



Supplement of

Influence of aerosol chemical composition on N₂O₅ uptake: airborne regional measurements in northwestern Europe

W. T. Morgan et al.

Correspondence to: W. T. Morgan (will.morgan@manchester.ac.uk)

1 Scope

The following supplementary material outlined in this document is provided to describe the revised calibration procedure for the Aerosol Mass Spectrometer, as well as incidental figures that support the main paper.

2 AMS calibration procedure

A problem was identified with the calibrations of the Aerosol Mass Spectrometer (AMS) used on board the FAAM research aircraft. The issue arose from a software bug from a custom built Differential Mobility Analyser (DMA) set-up, which led to the incorrect conversion of the raw data to absolute mass. This includes the RONOCO campaign, so a description of the correction is presented here.

A method for correcting the data has been formulated and this has been validated internally and shows consistency with the datasets that are unaffected by this problem. The size of the correction varies on a flight by flight basis. Described below is the detail of the correction.

The calibration is applied equally to all chemical species, so relative fractions or concentrations remain unchanged. As far as this manuscript is concerned, the correction only affects the absolute mass concentrations presented in Fig. 3 of the main manuscript and the calculation of water-to-nitrate and chloride-to-nitrate ratios for the Bertram and Thornton parameterisation. Given the agreement between the standard and alternative method of calibrating the AMS, the typical uncertainty assumed for the absolute mass concentrations is unchanged.

2.1 Background

The AMS requires several calibrations to convert the measured signal into mass. One of these calibrations determines the Ionization Efficiency (IE), which is the number of ions detected per molecule sampled. A full description of the calibration methodologies can be found in Jimenez et al. (2003) and Alfarra et al. (2004), which details how a calibration standard is converted to the IE. In brief, particles of a known size and chemical composition are generated and sampled by the AMS. These are normally dry, 350nm ammonium nitrate particles. The particles are size selected using a mobility based instrument, such as a Scanning Mobility Particle Sizer (SMPS). The validity of this method relies on the ability to accurately pre-size the particles with instruments such as the SMPS. It was found that for certain flights the flow rates in the SMPS were not set correctly and this led to a mis-sizing of the particles and the incorrect calculation of the IE. A new method to determine the particle size from the AMS data was devised.

2.2 Sizing using pToF mode data

Due to the bug in the DMA control software, the particles being delivered during calibration were of an unspecified and unknown size. The pressure-dependent size calibration method of Crosier et al. (2007) (following from Bahreini et al. (2003)) was

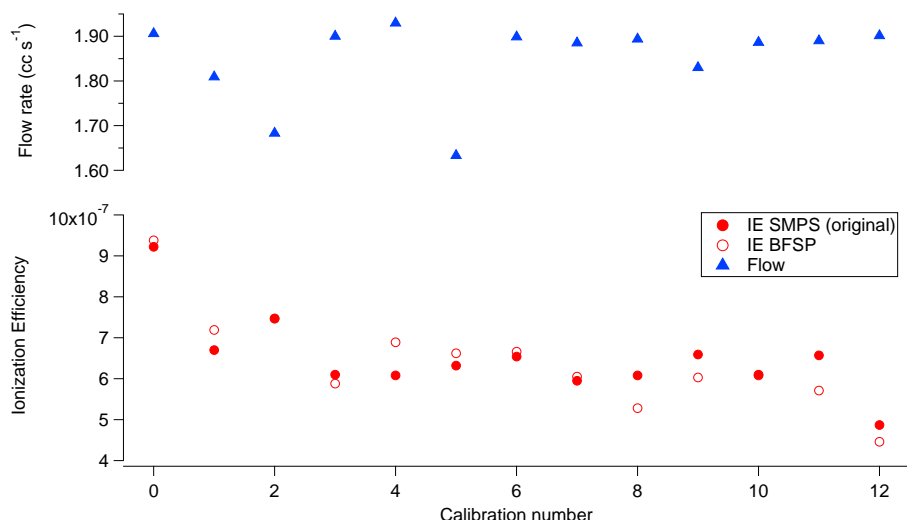


Figure S1: Original and recalculated IE using the Brute Force Single Particle (BSFP) method to determine D_m and flow rate from each calibration.

invoked to estimate the sizes based on particle Time-of-Flight (pToF) arrival times and measured inlet pressure, using the most recent calibration parameters available. The use of the pressure-dependent calibration accounted for changes in pinhole throughput (due to blockages and changes in temperature and pressure) and gave a more consistent IE/AB diagnostic than using the fixed-pressure calibration of Jimenez et al. (2003).

The median arrival time for each calibration was calculated and then in turn used to calculate the size of the aerosol measured by the AMS, D_{va} (vacuum aerodynamic diameter). This diameter is then converted to a mobility diameter, D_m , which is then used to calculate the IE. The mobility diameter was the diameter that was incorrectly reported due of the software bug.

2.3 Validation and results

To validate this approach, data from a campaign which was unaffected by the software bug was used. The re-calculated D_m and IE based on the method described above, were compared with the values used in the original analysis based on a D_m of 350nm from a working SMPS. The results are shown in figure S1 below and data summarised in Table S1.

The comparison of methodologies from a campaign unaffected by the mis-sizing yields an average IE ratio of 0.98. Therefore, the approach of using the arrival time of calibration particles in pTOF mode and a valid pressure dependent size calibration can be used in situations where the size of the calibration particles is unknown.

Table S1: Calculated values of IE and D_m from the original analysis and the alternative method.

Variable	Original	pTOF (Recalculated)
D_m (nm)	350	351.8 ± 9.79
IE	$4.41\text{e-}13 \pm 5.30\text{e-}14$	$4.34\text{e-}13 \pm 4.94\text{e-}14$

3 Box-model

As described in the main manuscript, an aerosol chemical box model (Lowe et al., 2009) was used to explore the validity of the steady-state assumption in these conditions. Fig. S2 shows the evolution of the $\text{N}_2\text{O}_5:\text{NO}_3$ ratio based on the expected ratio if the reaction is in equilibrium ($K_{eq}[\text{NO}_2]$) and based on the calculated NO_3 and N_2O_5 mixing ratios in the box model. Once emissions in the model have ceased and the sun has set, the two converge approximately 1 hour after sunset (around 2100L or 2000UTC), indicating that the system is in near-equilibrium and the steady-state assumption is valid. Consequently, we assume that when we sampled away from emission sources and it is an hour past sun set, the air parcels sampled by the aircraft are suitable for the steady-state analysis. See the main manuscript for further discussion.

Fig. S2 also includes a comparison between the measured $[\text{N}_2\text{O}_5]/[\text{NO}_3]$ ratio and when the ratio is calculated from $K_{eq}(T) \times \text{NO}_2$. Overall, the agreement is good with a slope of 0.94 between the measured and calculated ratios but there are some outliers.

4 Meteorological overview

A variety of air mass types were encountered during the two weeks of flying during the July RONOCO period, with the key synoptic meteorological features highlighted in Fig. S3 for reference. The beginning of the campaign was characterised by zonal flow from the west and relatively cooler temperatures and elevated wind speeds. From 20 July onwards, high pressure built over the UK region with the development of an anti-cyclonic system. This brought warmer air from continental Europe, particularly in the south-east of the UK and relatively low wind speeds. After this, a succession of frontal systems and associated precipitation passed over the UK, which reduced pollution concentrations. The end of the campaign saw north-westerly air flow across the UK due to the presence of a low pressure system over Scandinavia to the east of the UK and a high pressure system to the south-east. Temperatures were again cooler, although wind speeds remained relatively low compared to the beginning of the campaign.

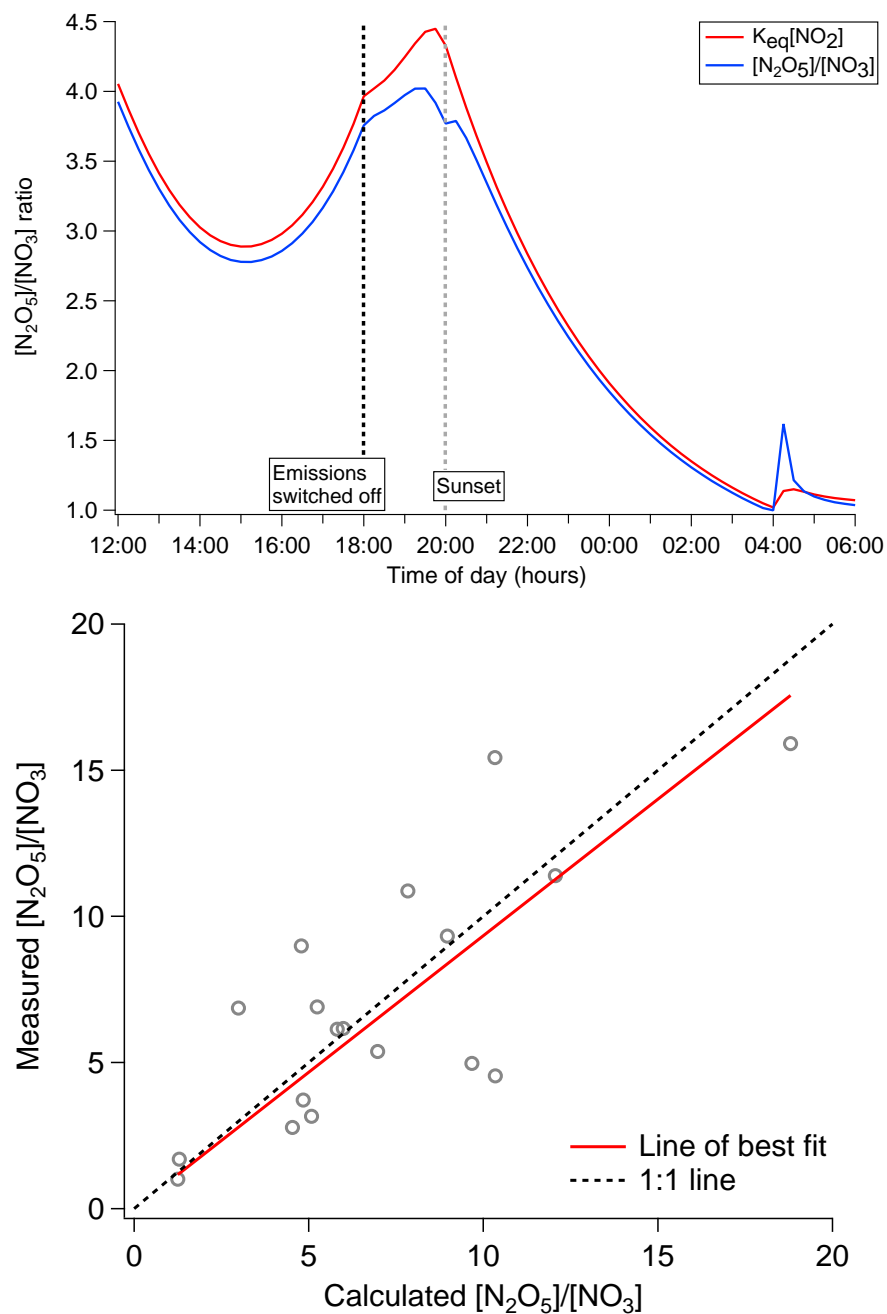


Figure S2: Top: Comparison between the evolution of the N_2O_5 and NO_3 ratio, assuming equilibrium ($K_{eq}[\text{NO}_2]$) and the modelled ratio based on aerosol box model simulations. Bottom: Comparison between the measured and calculated $[\text{N}_2\text{O}_5]/[\text{NO}_3]$ for the steady-state analysis case studies.

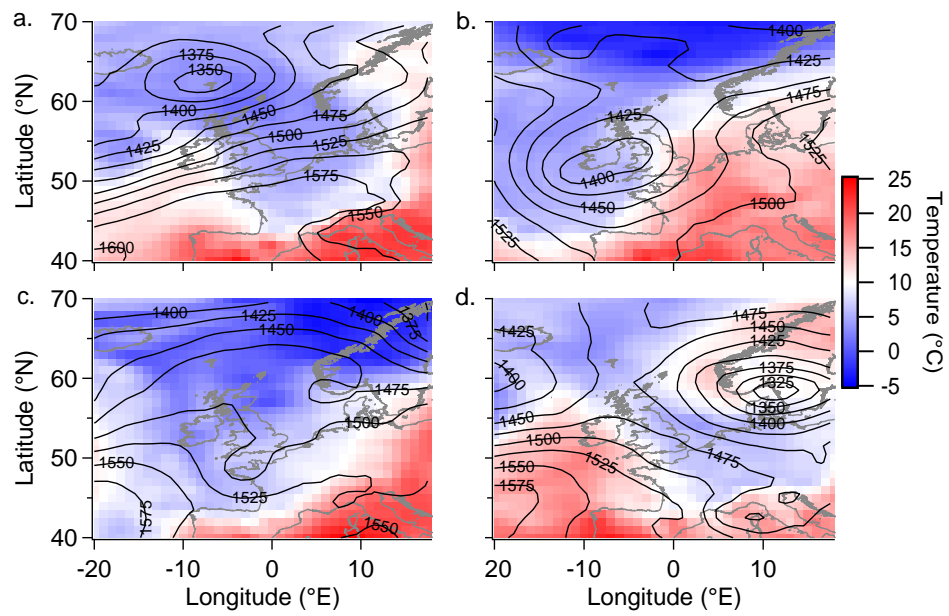


Figure S3: Meteorological summary for the July 2010 flying period. The contours represent the 850hPa geopotential height fields, while the colours are the ambient temperature at 850hPa. Panel (a) B535 - 18/07/10, (b) B537 - 21/07/10, (c) B538 - 23/07/10 and (d) B542 - 30/07/10. All panels are from 00:00 UTC.

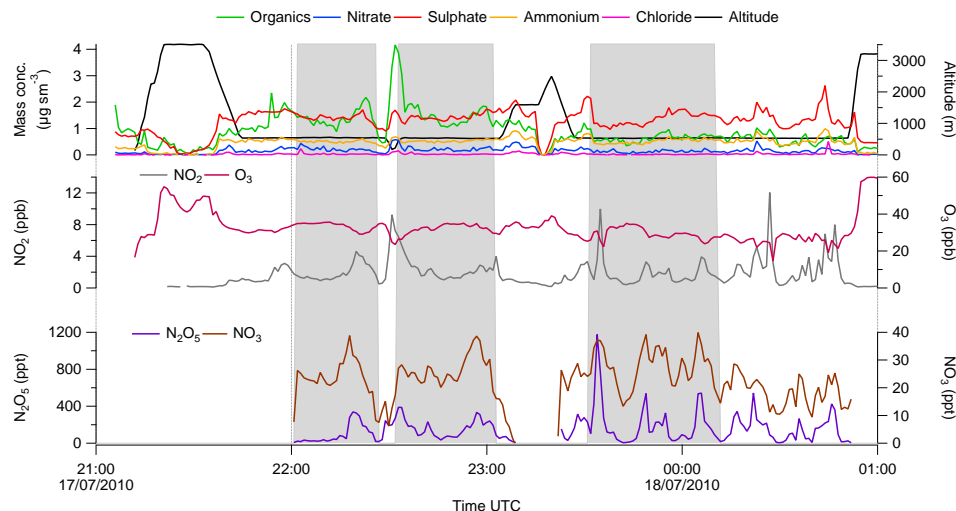


Figure S4: Time series of gas and particle phase measurements for flight B535. The altitude of the aircraft is also shown in the top panel. The grey shaded areas outline the periods used in the steady-state analysis.

5 Data Selection

Periods when the aircraft was conducting Straight and Level Runs (SLRs) were used for the N_2O_5 uptake analysis. These SLRs are typically 5-20 minutes long and this relatively short duration typically means that the pollution conditions are relatively homogeneous i.e. fairly constant aerosol concentrations and composition. An example of the periods selected for flight B535 is shown in Fig. S4.

References

- Alfarra, M. R., Coe, H., Allan, J. D., Bower, K. N., Boudries, H., Canagaratna, M. R., Jimenez, J. L., Jayne, J. T., Garforth, A. A., Li, S. M., and Worsnop, D. R.: Characterization of urban and rural organic particulate in the lower Fraser valley using two aerodyne aerosol mass spectrometers, *Atmospheric Environment*, 38, 5745–5758, doi:10.1016/j.atmosenv.2004.01.054, 2004.
- Bahreini, R., Jimenez, J. L., Wang, J., Flagan, R. C., Seinfeld, J. H., Jayne, J. T., and Worsnop, D. R.: Aircraft-based aerosol size and composition measurements during ACE-Asia using an Aerodyne aerosol mass spectrometer, *Journal of Geophysical Research*, 108 (D23), 8645, doi:10.1029/2002JD003226, 2003.
- Crosier, J., Allan, J. D., Coe, H., Bower, K. N., Formenti, P., and Williams, P. I.: Chemical composition of summertime aerosol in the Po Valley (Italy), northern Adriatic and Black Sea, *Quarterly Journal of the Royal Meteorological Society*, 133 (S1), 61–75, doi:10.1002/qj.88, 2007.
- Jimenez, J. L., Jayne, J. T., Shi, Q., Kolb, C. E., Worsnop, D. R., Yourshaw, I., Seinfeld, J. H., Flagan, R. C., Zhang, X. F., Smith, K. A., Morris, J. W., and Davidovits, P.: Ambient aerosol sampling using the Aerodyne Aerosol Mass Spectrometer, *Journal of Geophysical Research*, 108 (D7), 8425, doi:doi:10.1029/2001JD001213, 2003.
- Lowe, D., Topping, D., and McFiggans, G.: Modelling multi-phase halogen chemistry in the remote marine boundary layer: investigation of the influence of aerosol size resolution on predicted gas- and condensed-phase chemistry, *Atmospheric Chemistry and Physics*, 9, 4559–4573, doi:10.5194/acp-9-4559-2009, 2009.